Electronic Supplementary Material (ESI) for RSC Advances.

MICROVESICLE RELEASE AND MICELLAR ATTACK AS THE ALTERNATIVE MECHANISMS INVOLVED IN THE RED-BLOOD-CELL–MEMBRANE SOLUBILIZATION INDUCED BY ARGININE-BASED SURFACTANTS— SUPPORTING INFORMATION

Determination of surface-active properties

The effectiveness of adsorption (pC_{20}, the negative logarithm of the surfactant molar concentration required to reduce the surface tension of water by 20 mN.m^{-1}), the surface tension at the CMC (γ_{CMC}), the maximum surface-excess concentration (Γ_{max}) the maximum surfactant adsorption at the air-liquid interface), and the area per molecule (A_{min}) were also calculated from these plots through the use of the Gibbs absorption equation (Eq. 1):

$$\Gamma_{max} = -\frac{(\partial\gamma/\partial log C)}{2.303\, nRT} \quad (1)$$

where $\partial\gamma/\partial log\ C$ is the slope of the $\gamma/log\ C$ plot, n is the number of species in solution (for ionic surfactants, n = 2), T is the absolute temperature in degrees Kelvin (K), and R is the ideal-gas constant (R = 8.314 J.mol^{-1}.K^{-1}). The minimum area occupied per surfactant molecule adsorbed at the air-liquid interface (A_{min}), expressed in Å^2, was also calculated according to equation (2):

$$A_{min} = 10^{16}/N_A\Gamma_{max} \quad (2)$$

where 10^{16} is the conversion factor from cm^2 to Å^2, N_A is the Avogadro's number and Γ_{max},

the maximum surfactant adsorption, is expressed in mol.cm^{-2}.

Surface-tension measurements also enabled the determination of other relevant parameters related to the surfactant's surface properties (A.T. Florence and D. Attwood, *Physicochemical Principles of Pharmacy,* 4th edn., Pharmaceutical Press, London, 2006). Table S1 summarizes the above parameters together with the γ_{CMC} and pC_{20}, which values are commonly employed as indicators of the respective effectiveness and the efficiency of adsorption of the surfactants. A lower γ_{CMC} indicates a higher effectiveness of the surfactant in reducing the surface tension. The greater the pC_{20} value, the more efficient is the surfactant—*i. e.*, a lower concentration is needed to decrease by 20 units the surface tension of pure water. The two Bz-Arg-NHC$_n$ gave γ_{CMC} values ranging from 30 to 37 mN.m^{-1}, which figures are considered typical for quaternary surfactants, including arginine-based ones.

Table S1. Surface-active properties of Bz-Arg-NHC$_n$ (single-chain surfactants derived from arginine) at 25 °C

Bz-Arg-NHC$_n$					
n	**CMC** (mM)	γ_{CMC} (mN.m^{-1})	pC_{20}	Γ_{max} (x 10^{-10} mol.cm^{-2})	A_{min} (Å^2)
10	0.23	34.0	3.17	3.03	54.8
12	0.085	36.8	4.47	3.53	47.0

n, *N*-alkyl carbon-chain length

Solubilization of erythrocyte membrane: determination of the surfactant/lipid ratio

Lichtenberg's model (reference [18] in the manuscript) describes the action of surfactants on lipid membranes as a complex process that comprises at least three steps. During the first, when the surfactant is present at subsolubilizing concentrations, the molecules would partition between the aqueous medium and the membrane. At higher surfactant concentrations, micellization would occur and the surfactant-saturated membranes would coexist with lipid-detergent mixed micelles. Finally, when the surfactant concentration exceeds that required for complete solubilization, all surfactant-enriched–membrane fragments turn into small mixed micelles. In the example of membranes composed of phospholipids, cholesterol, and integral proteins; the formation of mixed aggregates could also be evidenced in the presence of surfactants. The structure of these assemblies depends on the molar ratio of soluble to insoluble amphiphiles (R_e): below a critical value (R_{sat}) the mixed assemblies are lamellar, whereas above another critical ratio (R_{sol}) the membranes become surfactant-lipid-protein mixed micelles.

In each instance, D_{sat} and D_{sol} values were established as the respective surfactant concentrations required to reach saturation (the onset of hemolysis) and to induce total membrane solubilization (total lysis). Finally, the D_{sat} and D_{sol} values for the different erythrocyte concentrations were plotted as a function of the lipid concentration in each erythrocyte suspension. The data are fitted to a straight line as follows Eq. (3):

$$D_t = R_e \times \left(L + \frac{1}{K_b\,(R_e + 1)} \right) \qquad (3)$$

where D_t is the total surfactant concentration (D_{sat} or D_{sol}) and L is the lipid concentration in the system. The slope of the resulting straight lines enables the calculation of R_e (R_{sat} or R_{sol}), while the y-intercept corresponds to the concentration of free detergent in water, D_w. Finally,

K_b (M^{-1}), the molar binding constant of the surfactant to the erythrocyte membrane at saturation, can easily be derived from Eq. (4):

$$D_w^{sat} = \frac{R_e}{K_b^{sat}(R_e + 1)} \quad (4)$$

In order to establish the role of the surfactant monomers in membrane solubilization, we studied the hemolysis of HRBCs by the two lipoamino acids at 4 different hematocrits: 0.075, 0.15, 0.30, and 0.45% (v/v; Fig. S1).

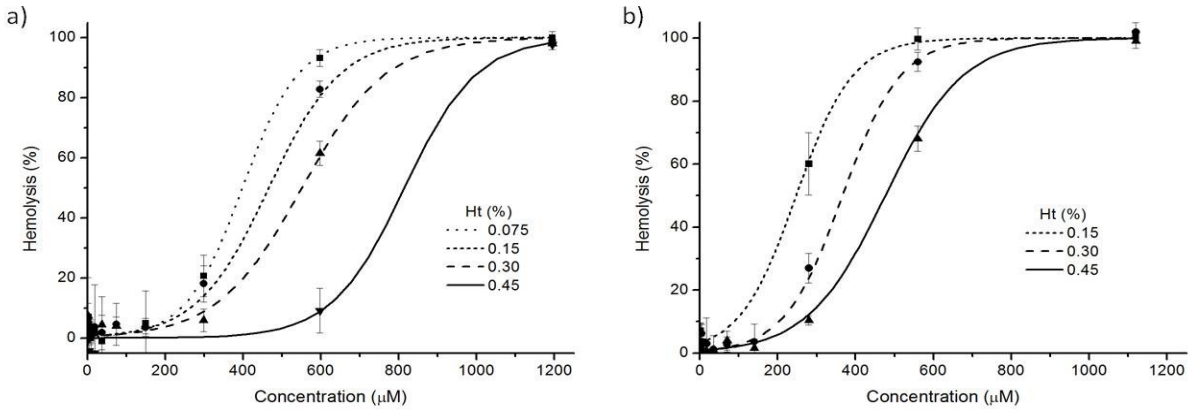

Fig. S1 . Hemolysis of HRBCs after incubation with Bz-Arg-NHC_{10} (Panel a) and Bz-Arg-NHC_{12} (Panel b) in isotonic PBS buffer pH 7.4 for 1 h at different hematocrits (Hts). In the figures, the percent hemolysis is plotted on the *ordinate* as a function of surfactant μM concentration. Key to Hts indicated by the curve textures: dotted, 0.075%; short-dashed, 0.15%; long-dashed, 0.30%; solid, 0.45%

D_t values (*i. e.*, D_{sat}, and D_{sol}) were calculated from each dose-response curve and plotted as a function of erythrocyte-membrane-lipid concentration (Fig. S2, triangles and squares, respectively).

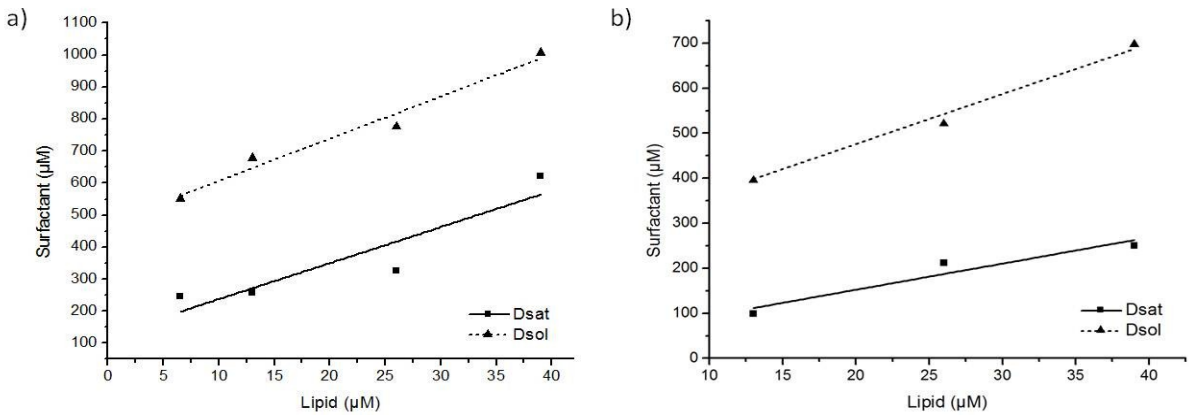

Fig. S2. Total μM concentration of the surfactants Bz-Arg-NHC_{10} (Panel a) or Bz-Arg-NHC_{12} (Panel b), plotted on the *ordinate*, needed for membrane saturation and total solubilization—*D*sat (squares) and *D*sol (triangles)—as a function of the erythrocyte-membrane-lipid μM concentration indicated on the *abscissa*.

Fig. S2 illustrates the direct correlation between D_t and the lipid concentration found for both arginine-based surfactants, as the values increased with the elevation in membrane-lipid concentration. In all instances, the D_{sat} and D_{sol} values obtained for Bz-Arg-NHC_{10} were higher than those calculated for Bz-Arg-NHC_{12}. As described above, from these plots the effective surfactant/lipid molar ratios (R_e) for saturation and total solubilization (R_{sat} and R_{sol}) as well as the corresponding concentration of free detergent in water (D_w^{sat} and D_w^{sol}) were established for each surfactant. Table S2 summarizes the parameters obtained.

Table S2. Effective surfactant/lipid molar ratios (R_{sat} and R_{sol}), free surfactant concentration in water (D_w), and binding constant (K_b) in the lysis of human erythrocytes by the two Bz-Arg-NHC_n

	Bz-Arg-NHC_{10}	**Bz-Arg-NHC_{12}**
$\boldsymbol{R_{sat}}$	11.26	5.81
$\boldsymbol{R_{sol}}$	13.18	11.6
$\boldsymbol{D_w^{sat}}$ (mM)	0.125	0.036
$\boldsymbol{D_w^{sol}}$ (mM)	0.475	0.235
$\boldsymbol{K_b^{sat}}$ (M^{-1})	0.0073	0.0235

Another fundamental parameter to consider is the free amount of surfactant in water (D_w), which value can be interpreted as the CMC of the compound in the presence of a lipid membrane. As seen from the data in Table S2, the D_w^{sat} values were 1.8 and 2.3 times lower than the respective CMCs for Bz-Arg-NHC_{10} and Bz-Arg-NHC_{12}, thus demonstrating the affinity of the surfactants for the erythrocyte membrane.

Kinetics of hemolysis

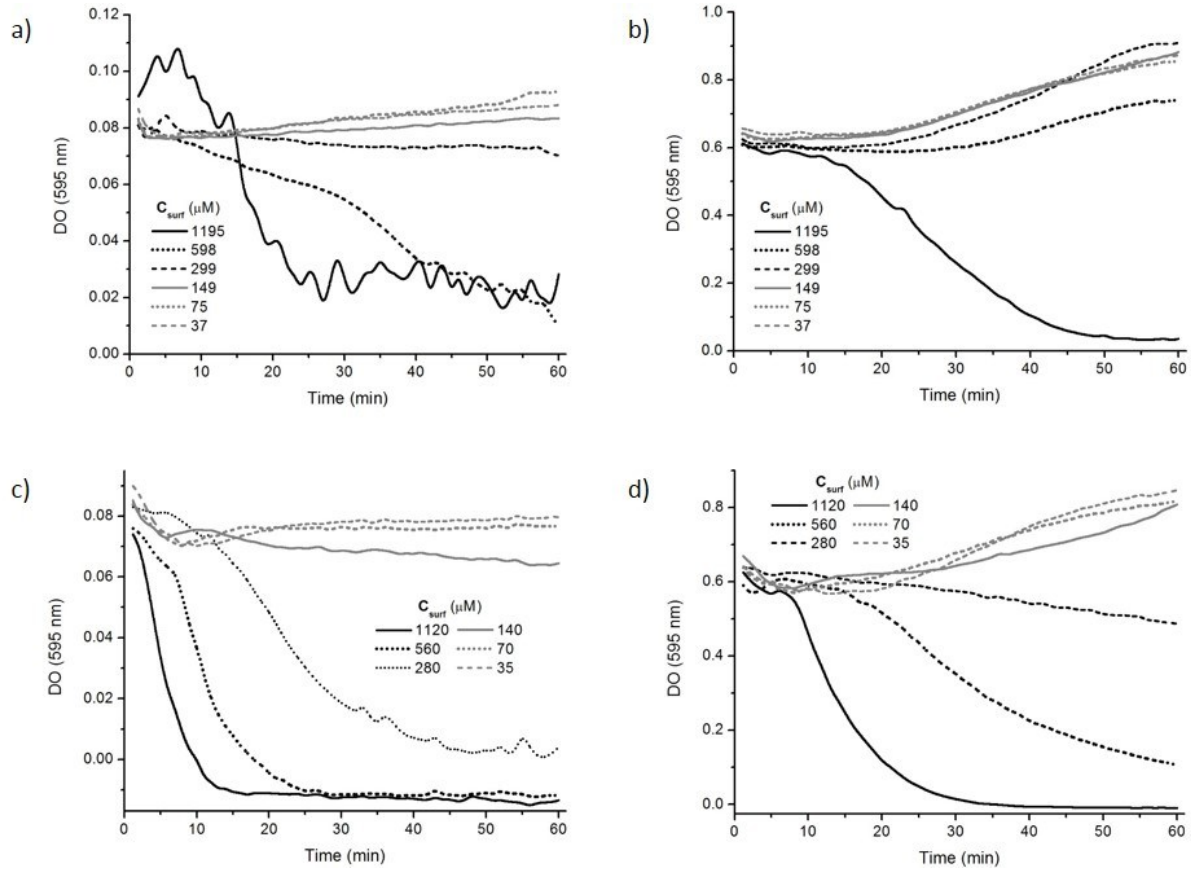

Fig. S3. Hemolysis kinetics of human red blood cells by Bz-Arg-NHC_{10} (panels a and b) and Bz-Arg-NHC_{12} (panels c and d) at hematocrits of 0.075% (panels a and c) or 0.45% (panels c and d). In the figures, the kinetics of hemolysis as measured by changes in optical density at 595 nm is plotted on the *ordinates* as a function of time in min on the *abscissas*. Key to curve textures indicating surfactant concentrations (μM): (panels a and b) solid black, 1,195; dotted black, 598; dashed black, 299; solid gray, 149; dotted gray, 75; dashed gray, 37; (panels c and d) solid black, 1,120; dotted black, 560; dashed black, 280; solid gray, 140; dotted gray, 70; dashed gray, 35.